European networks observing the atmospheric boundary layer: Overview, access and impacts

Chapter: Doppler lidar (DL)

Document version	**1.3**
Version date	**06/2024**
PROBE deliverables	**3.1, 3.3, 4.1, 4.2**
Authors	Document preparation conducted by Ewan O'Connor and Jana Preissler Authors: Ewan O'Connor, Markus Kayser, Volker Lehmann, Maxime Hervo, Clément Toupoint, Christopher C. Holst, Sven-Erik Gryning, Ekaterina Batchvarova, Jonnathan Céspedes, Emilia Bertonasco

COST Association AISBL | Avenue Louise 149 | 1050 Brussels, Belgium
T +32 (0)2 533 3800 | F +32 (0)2 533 3890 | office@cost.eu | www.cost.eu

Funded by the Horizon 2020 Framework Programme of the European Union

Contents

Introduction

This report provides an overview of operating Doppler lidar (DL), including introduction to sensor, products, manufacturers, instrument types, instrument setup and required regular maintenance on site, calibration, measurement configuration, data formats, QA/QC methods and retrieval methods.
The structure of the document follows the deliverable requirements of PROBE. Part 1 gives a general overview of Doppler wind lidars and their application and products. Part 2 refers to instrument operations, including instrument setup, required maintenance, calibration and measurement configuration (PROBE deliverable D4.1). Part 3 is introducing data formats, and quality control methods (PROBE deliverable D3.1). Part 4 is listing retrieval methods and shows advances in data assimilation (PROBE deliverables D3.3 and D4.2).

Part 1 General overview

Introduction

Doppler lidars observe the radial (line-of-sight, LOS) Doppler velocity of atmospheric tracers such as molecules or aerosol using direct detection methods, typically at UV wavelengths, or by coherent heterodyne detection, typically using IR wavelengths within the atmospheric window regions. Hence, the latter method offers advantages for ground-based systems to observe the atmospheric boundary layer, while the former, using molecules as tracers, is best suited for space-based or airborne operations to measure radial velocities in the upper troposphere, stratosphere, and mesosphere (Reitebuch, 2012).
Most commercial systems employ solid-state fibre-optic technology and coherent heterodyne detection, with the tracers being aerosol, cloud droplets, or ice particles. Two implementations are available for these robust and low-powered systems: pulsed (Pearson and Eacock, 2002), and continuous-wave (CW) (Pitter et al., 2015). CW systems obtain the range information by adjusting the telescope focus to change the range-weighting function and are suitable for operation up to about 300 m in altitude. Pulsed systems, similar to automatic lidars and ceilometers (ALCs), use the time-of-flight to obtain range information. Pulsed systems are necessary to cover the full depth of the boundary layer. The fibre optic design allows a high degree of flexibility, and these instruments are available in a number of guises: vertical stare only, full all-sky scanning capability, scan within a conical zone, or optimised for winds only. Some systems operate at very high pulse rates and average many pulses to achieve the required sensitivity, whereas others may operate at lower pulse rates, but with larger per-pulse energies. Like ALCs, commercial systems can operate autonomously and require little maintenance.

Products

The raw quantities typically retrieved by Doppler lidar systems are signal power and the radial Doppler velocity. Some systems can also be configured to provide the signal power spectrum (from Fast Fourier Transform, FFT, or from lagged-autocorrelation) from which Doppler spectra can be produced (Pearson et al., 2009). If the telescope function (the function of the change of effective receiver area with range) is known or calculated, the signal profile can be converted into a profile of attenuated backscatter coefficient (Pentikäinen et al, 2020).
The vertical profile of horizontal wind is then retrieved from a combination of scans using trigonometry. Scan types for single Doppler lidar retrievals include Doppler Beam swinging (DBS) similar to sodars and radar wind profilers or conical Velocity-Azimuth-Display (VAD) scans at a constant elevation angle (Päschke et al., 2015; Teschke et al., 2017). Other possibilities include the use of two or three systems operating together to create virtual-towers (Debnath et al., 2017; Lane et al., 2013; Calhoun et al. 2006). The presence of wind shear and low-level jets (LLJ) can then be diagnosed from the retrieved wind profiles (Tuononen et al., 2017; Pichugina et al., 2012; Céspedes et al., 2024). See Appendix A for application examples on LLJ.
Turbulent characteristics can be derived from the rapid velocity fluctuations, both from vertical and from scanning operation (Bonin et al., 2017; Smalikho and Banakh, 2017; O'Connor et al. 2010).

Further, a boundary layer classification can be generated from the combination of the horizontal wind profiles, turbulent characteristics and attenuated backscatter profiles (Krishnamurthy et al., 2021; Bonin et al. 2018; Smalikho and Banakh, 2017; Manninen et al., 2018; Harvey et al., 2013; Tucker et al., 2009). See Appendix B for application examples on turbulence parameters.

Manufacturers/Instrument types

Table 1 lists manufacturers and instrument types relevant for boundary layer profiling. A broader range of instruments exists for shorter range wind detection, as is relevant for wind energy or other applications. All instruments considered in Table 1 transmit at a wavelength close to 1.5 µm.

Table 1: Overview of commercial long-range Doppler lidars

Manufacturer	Instrument	Scanning	size/weight	PRF
Vaisala (former Leosphere)	WindCube Scan (100S, 200S, 400S)	Hemispheric	compact 250 kg	> 10 kHz Depends on operating mode
Halo Photonics	Streamline, Streamline XR	Hemispheric	compact 60 - 85 kg	> 10 kHz Depends on manufacturer setup
	Streamline Pro	Limited cone (20 degrees)	65 kg	> 10 kHz Depends on manufacturer setup
Mitsubishi Electronic	Terminal DL	Hemispheric	small container 2000 kg	250 Hz
Leonardo	Skiron 3D	Hemispheric	small container 3500 kg	4 kHz
Lockheed Martin	Wind Tracer	Hemispheric	small container 1600-2500 kg	750 Hz

Part 2 Instrument operations (PROBE D4.1)

Instrument setup

As can be seen from the list of manufacturers and instruments in Table 1, there are two size classes of instrument. Those which are container-based will require a levelled platform or rooftop capable of supporting significant weight and an access area approaching 5 by 5 metres. The smaller size class, compact, comprises standalone instruments for which a stable surface is required, but an uneven surface can be compensated for by the adjustable legs/feet. The small instruments may also need fixing to the surface with suspension straps.

The deployment environment surrounding should have at least an open view within a cone of specified angle from zenith, in order to perform conical scans for the retrieval of the horizontal wind profile, and ideally an open view to the horizon in all directions to enable low-elevation scans. The instrument should be aligned to a reference (preferably North). Additionally, the operator has to assure that the lidar is levelled accurately.

The instrument should be kept powered continuously as this will keep the instrument internal temperature stabilised. An accurate system clock is also necessary, which can be achieved using a time server (e.g. ntpd) or a GPS reference. Most commercial systems now include an internal GPS reference as standard. More considerations for standard operating procedures are given in Table 2.

The near-IR wavelength of operation permits eye-safe use, but operation may require permission in some locations.

Required regular maintenance on site

Preventive maintenance is limited to occasional cleaning of the telescope. Vaisala (former Leosphere) systems may need a regular change of desiccant to prevent the internal fogging of the telescope lens in damp conditions and regular lubrication of the scanner head. Over longer-term operation (5-10 years), some components may need replacement, such as amplifiers and the scanning motors, bearings or housing as well as the internal computer or hard-drives.

Calibration

Calibration is facilitated by a co-located ceilometer for an extended period to determine telescope focus function if use of attenuated backscatter profile is required (Pentikäinen et al., 2020). Besides, regular hard-target measurements, e.g. using a nearby wind turbine or mast, to keep track of potential systematic biases in pointing angle, range offset or Doppler velocity are recommended.

Table 2: Considerations for standard operating procedures

Retrieval of Calibration Parameters	• Calibration parameters: absolute calibration, background correction, telescope function and variability • Absolute calibration: - Doppler velocity and range calibration: hard target check - Attenuated backscatter: liquid cloud technique, after telescope focus determination. • Background correction performed during standard processing. • Telescope function determination by comparison with co-located ceilometer. Required every time telescope focus changed, or instrument modified/upgraded.
Characterization of measurement uncertainties	• **Doppler velocity uncertainty sources:** - Offset uncertainty assessed during instrument calibration and hard target. - Signal to noise ratio (including variation in laser power) • **Wind uncertainty sources:** - Pointing angle uncertainty - Doppler velocity uncertainty - Turbulent and inhomogeneity uncertainty • **Attenuated backscatter uncertainty sources**: - SNR uncertainty (including background correction uncertainty) - Telescope focus uncertainty - Cloud calibration method uncertainty
Calibration schedule (automatic and hands-on)	• Automatic processing for SNR and velocity uncertainty. Cloud calibration updated every event. Telescope focus can be continuous or periodic depending on co-located ceilometer availability
Azimuth and elevation pointing accuracy	• For scanning instruments (target and/or horizontal winds). Provide azimuthal correction from north. Ensure horizontal alignment of instrument.
Detecting systematic errors during instrument operation	• Hard target velocity calibration and pointing angle (target and/or horizontal winds). • Monitor instrument stability (background, telescope focus, cloud calibration)

Measurement configuration

The scanning capability of these instruments implies that the configuration can be optimised for the location and application requirements as detailed in the retrieval method section. Network operation may include specific requests, for example, ACTRIS recommends that these are included within the scan schedule:

- Vertical scanning
  - High temporal resolution (< 5 seconds if possible)
  - Provides
    - Vertical air motion
    - Turbulent parameters,
    - Diagnosis of aerosol, cloud, precipitation
- Conical scanning
  - VAD with at least 12 beams, or continuous scan mode (CSM)
    - Trade-offs between scan time and retrieval robustness determine number of beams
  - At two elevation angles if possible
    - 50-75 degrees elevation angle (15-40 degrees from zenith) for full extent of boundary layer
    - shallow elevation angle for capturing shallow boundary layers
  - One full scan every 15 minutes or less
    - Provides winds

Number of beams in Velocity Azimuth Display (VAD) scans

The retrieval of wind data from conical scans is affected by definitions of averaging time scales, in which vector- (per scan) or scalar- (cumulative) averages can be calculated. The number of beams per scan is an important parameter for vector averaging, because a larger number of beams can provide uncertainty bounds for the scan accuracy and affect robustness of retrieval. For 24 beams, 8 times more samples than required to mathematically close the equations are obtained. This redundant sampling leads to normally distributed errors cancelling out, as visualised in Figure 1. The drawback of more beams is the extra time needed to complete a scan. The Metek Windranger system, for instance, samples VAD scans every second with 100 beams each, but focuses on a single measurement height for each scan. HaloPhotonics StreamLine systems typically require approximately 100-150 seconds for 24 beam scans but sample the entire profile simultaneously. The optimum could be 12 to 24 beams, depending on site specific factors, stationarity time scales of the wind field, and scheduling restrictions due to intended applications of the data.

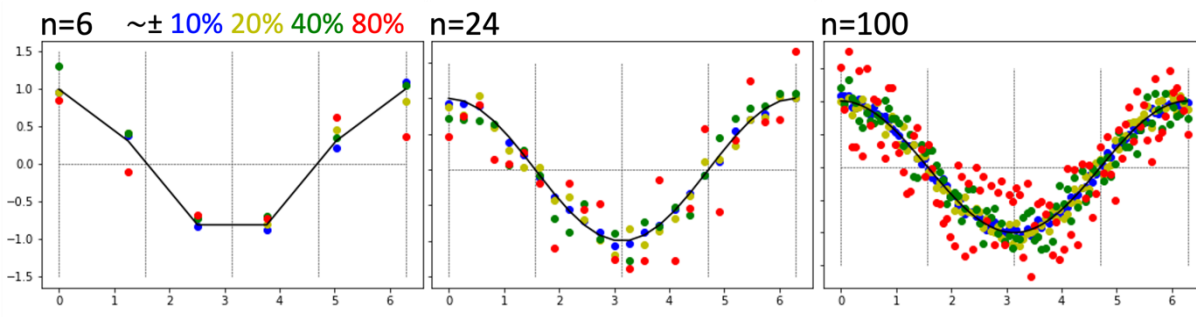

Figure 1: Synthetic data to demonstrate the effect of normally distributed noise depending on the number of beams for VAD retrievals. The relative magnitude of the noise is colour-coded as indicated at the top of the graph, while the black line refers to a simple cosine function.

VAD Scan variations were analyzed using the data collected by five DL systems measuring with 6, 8, 12 or 24 directions (Bertonasco and Kayser, 2024). To achieve better comparability among the instruments, all data sets are adjusted to the RWP as a reference by fitting a linear function and

correcting the data accordingly. One can find that VAD 12 and 24 yield a smaller MSE than VAD 6 and 8, matching the results of (Teschke and Lehmann, 2017). The results disagree with (Rahlves et al., 2022), where it is stated that poor performance of horizontal wind speed measurements is found for the VAD 24 scheme in conjunction with an elevation of 75° and that in most of the analyzed cases, the VAD 6 proves superior to VAD 24 for horizontal wind speed measurements. Further, the results presented here suggest that 12 directions perform as good as 24. Hence, this study recommends 12 directions for use in operational networks. But in this regards, additional experiments should be performed. It would be interesting to extend the study, setting up even more DL systems and testing for a higher variety of numbers of directions e.g. also for 10, 16, and 20 as well as different elevation angles.

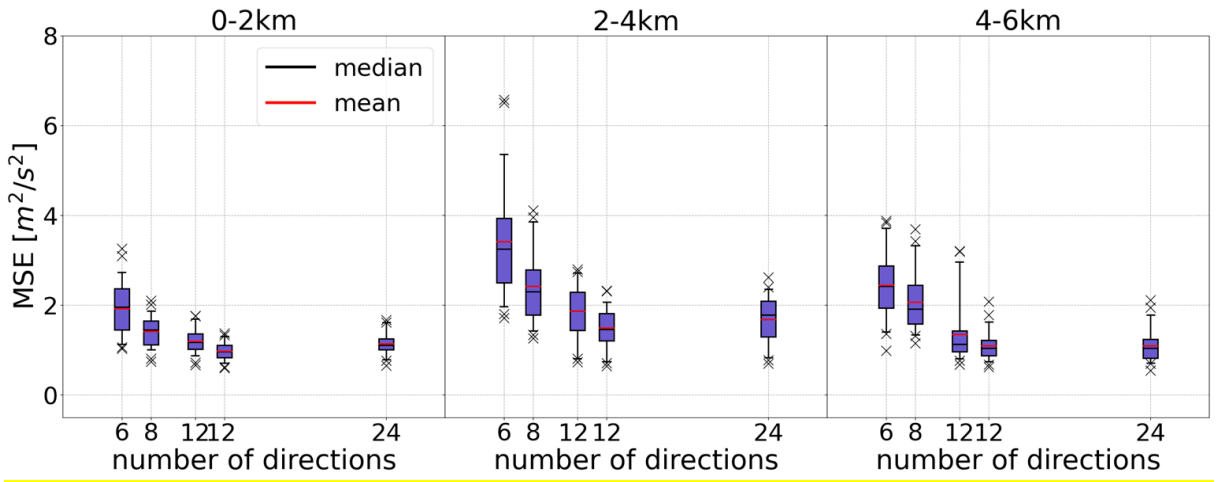

Figure 2 Results of a field test performed at the Meteorological Observatory Lindenberg with Doppler lidars using VAD scans with different number of directions: Mean square deviation (MSE) of the winds between co-located Doppler lidars and the radar wind profiler at Lindenberg as a reference. The results are split into three height regions.

Shallow DBS

The Shallow DBS is a scan strategy developed to extend the vertical profile of the horizontal wind downward into the region of the blind zone of a Doppler lidar, in this example the Vaisala WindCube Scan 400, that defines the height of the first available level from the classical Doppler Beam Swinging (DBS) retrieval when scanning at a common elevation angle of e.g. 75 degrees. Currently, a DL is operating at the QUALAIR-SU measurement site in central Paris on the rooftop of a tall building (Zamansky Tower, 88 m). This means that the first available DBS retrieval product level is 238 meters above the city. Adding information from a shallow DBS (elevation of 10 degrees), the first data point of the horizontal wind profile is brought down to 128 m. This new profile provides new insight into the near-surface interaction between the wind flow and the urban surface.

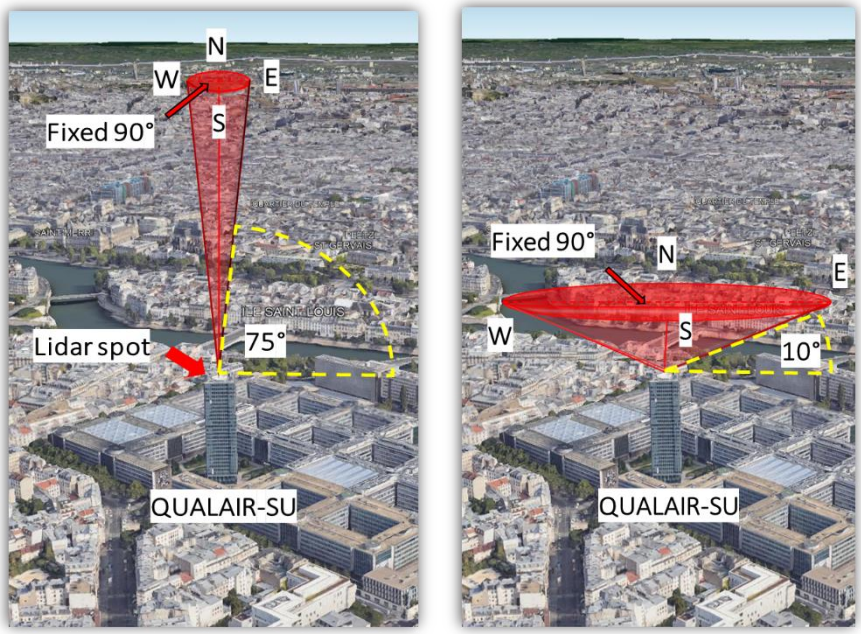

Figure 2. Schematic representation of a) the classical Doppler Beam Swinging (DBS) scan strategy of the Vaisala WindCube Scan 400s, and b) the shallow DBS scan strategy. Note the elevation angle for classical DBS is 75° and for the shallow DBS is 10°.

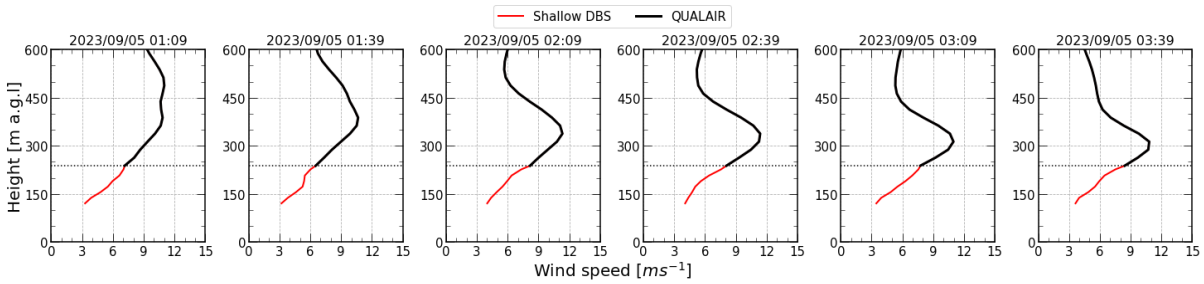

Figure 3. Examples of vertical profiles of horizontal wind speed measured by the classical DBS scan (solid black curves) and the extended fraction retrieved by the shallow DBS scan (red curve). The horizontal dotted line represents the altitude (238 m above the city) of the first available range gate of the classical DBS.

Part 3 Data and format standards

Data formats

The data formats vary from manufacturer to manufacturer. It is recommended to always store the data in the native manufacturer format in the first instance.

Figure 4 outlines the processing steps that are performed by a coherent Doppler lidar in order to obtain the calibrated data necessary for calculating meteorological parameters. Processing up to *Calibrated data* is usually performed by the instrument internally in real time. Access to *raw timeseries* is often not possible as these are discarded immediately after on-board processing; if stored, the typical daily volume would easily exceed 1 terabyte. Access to *Raw spectra* is usually possible from most instruments, although archiving of this data is often not switched on by default.

The ACTRIS network requires the *Calibrated data* in the native format for central processing at the ACTRIS data centre, and will use the housekeeping data for QA/QC. However, for use in an operational network that might include different system types and systems from different manufacturers, it may be more appropriate to archive data in a common format that is compatible with the CF-standard.

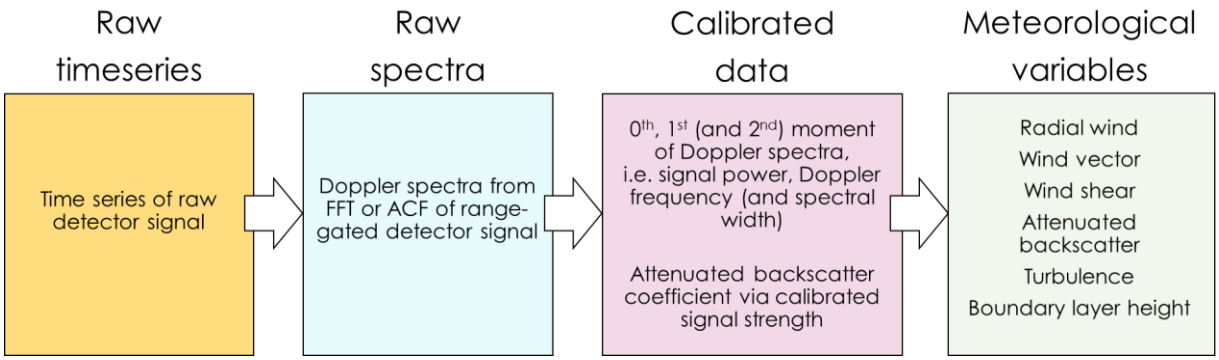

Figure 4: Processing steps for coherent (heterodyne) Doppler lidar systems.

The current native *Calibrated data* formats are:

- Vaisala (former Leosphere) – long-range WindCube Scan systems
  - .nc: calibrated signal and radial velocity files, including some housekeeping data
    - Note that these are in HDF5-netcdf4 format, which includes groups, see CF-radial
- Halo Photonics Streamline systems
  - .hpl: calibrated signal and radial velocity files
  - .txt: housekeeping data
    - system_parameters_*.txt
    - Time_sync_*.txt
    - Background_*.txt
  - .acf: raw spectra (complex autocorrelation function, ACF)

Spectral files are available from Vaisala systems, and from Halo Photonics systems (.acf files), but as stated previously, recording of these is not on by default due to the large data volume.

QA/QC methods

All instruments store the instrument setup specification data (transmission, acquisition, integration parameters) including those that can change with scan type and scanning parameters in the housekeeping data.

In addition, the instrument internal temperature and humidity logs, together with background noise files for certain instrument types, should also be recorded. Background noise data is used for automated quality control and correction (Manninen et al. 2016), which can be augmented with internal temperature information. Temperature and humidity logs are also used in examining drifts and biases, and for identifying possible fogging/freezing of the telescope lens.

Doppler lidar range and atmospheric conditions

Doppler lidars provide valuable data for several applications. For all these uses, the remote sensing capability of wind lidars is crucial to probe large volumes of the atmosphere. However, the performance of wind lidars depends on many environmental factors and can vary significantly depending on the location and conditions on site.

Indeed, the characteristics of the return signal of remote sensors depend directly on the state of the atmosphere, which is based on several variables such as extinction, backscatter, temperature, and more. Although the effect of some of these variables is generally understood, such as precipitation or fog that limit the measurement range of the lidar due to increased atmospheric absorption, the effect of many atmospheric parameters still has to be qualified and quantified precisely.

Temperature gradients in the air modify the optical index of the air, which in turn affects the transmission of electromagnetic waves. In parallel, aerosols that backscatter the lidar signal are affected by humidity, which can modify their backscattering properties.

By using conditional statistics, we highlight the effect of these variables on the measurement range of a Doppler wind lidar. We show that the performance of the lidar is affected by daily variations along these variables, superimposed on a slower evolution, that depends on other atmospheric parameters.

Further development could lead to a finer prediction of the measurement range depending on the location of the device, thus helping users to plan and predict their measurement acquisition more efficiently.

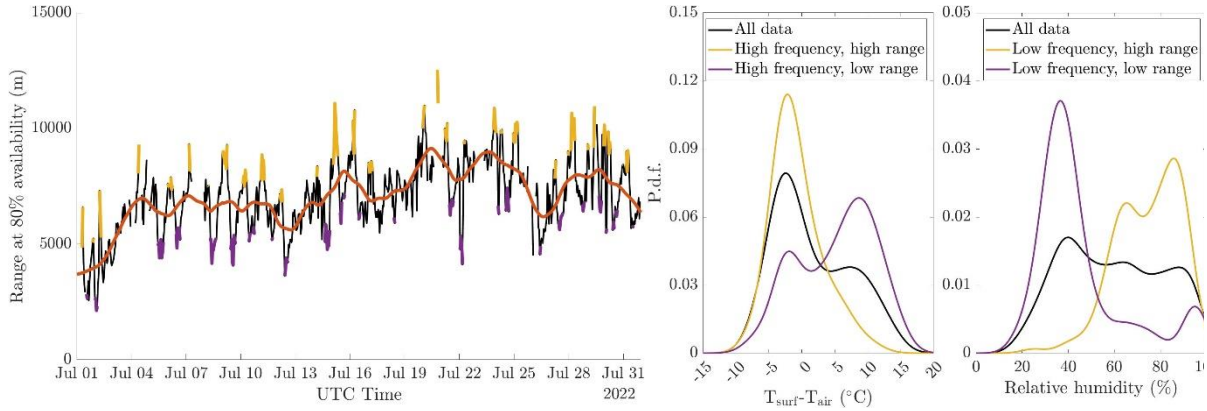

Figure 5: Conditional statistics of temperature gradient and relative humidity in relation with lidar range.

Behaviour of data availability and carrier to noise ratio (CNR) of a Doppler lidar in Northern Greenland

Results from the operation of a Doppler wind lidar in the high Arctic show that close to the ground there is a pronounced annual variation, with high aerosol concentrations (large CNR values) during winter and orders of magnitude smaller during summer. Due to this meteorological effect, the conditions for the operation of the Doppler wind lidar are less favorable during summer.

We investigated the relationship between the CNR and the mean horizontal wind speed estimated by the lidar using raw one-Hertz data. We applied a threshold value for the CNR of the individual wind speed observations and composed a mean horizontal wind speed for the range of CNR threshold values between -32 dB and -14 dB. The effect of the filtering was found to be very different along the range of CNR values. Figure 6 shows the mean horizontal wind speed normalized with the mean wind speed for the highest CNR value (-14 dB) as a function of CNR. Thus, the normalized wind speed is one for a CNR threshold value of -14 dB. High values of the CNR represent a high concentration of particles that backscatter the light beam. High values of the CNR indicate therefore observations of the wind speed with high accuracy, and decreasing values of the CNR gradually give rise to a higher uncertainty (Gryning & Floors 2019).

For the Doppler lidar used in this study there is a flat plateau between -26 and -22 dB in which the estimate of the wind speed is not sensitive to the choice of the CNR threshold value. The extent of the flat plateau is instrument dependent and the height dependency remains to be investigated. The abrupt increase in the normalized wind speed for CNR values lower than -26 dB is where the backscattered signal becomes weak due to low aerosol concentrations and noise starts to corrupt the estimation of the mean wind speed.

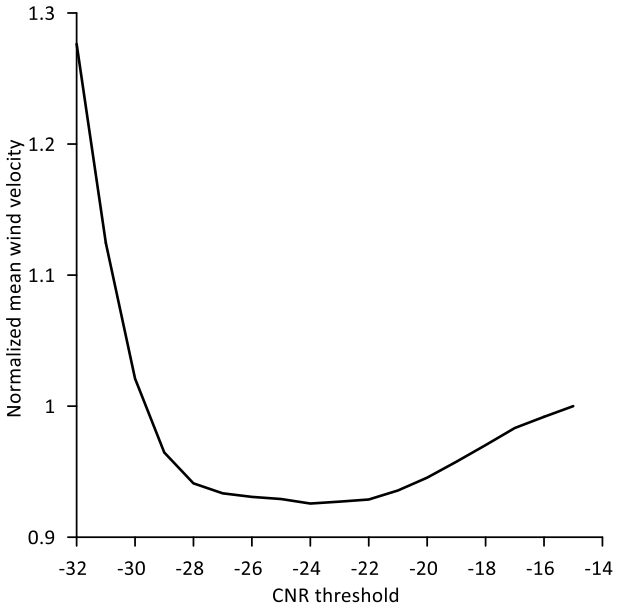

Figure 6: Illustration of the normalized mean wind velocity as a function of the Carrier-to Noise ratio. The data represent 10-min average observations from 2018 with a measuring height of 100 m. The normalization is performed with the mean wind speed corresponding to a CNR threshold value of -14 dB.

Part 4 Data processing

Retrieval methods

There are numerous methods in the literature for retrieving meteorological and other geophysical parameters from the Doppler lidar systems described in this document. A detailed description of the methodologies used for retrieving each meteorological product is given in the references in Table 3.

Table 3: References for retrieval methods

Meteorological product	Description	References
Winds	DBS scan VAD or CSM VAD or CSM Virtual Tower	Lane et al., 2013 Päschke et al., 2015 Teschke and Lehmann, 2017 Calhoun and Heap et al., 2003 Debnath et al., 2017
Wind shear	From wind product	Pichugina et al. 2012
Low Level Jet (LLJ)	From wind product	Tuononen et al., 2017
Turbulence	Vertical stare VAD, 6-beam, RHI VAD (CSM) VAD	O'Connor et al., 2010 Bonin et al., 2017, 2018 Smalikho and Banakh, 2017 Vakkari et al., 2015
Wind gust	rapid CSM	
ABL	Threshold retrieval Machine learning approach	Schween et al., 2014 Krishnamurthy et al., 2021
ABL classification	Combine winds, turbulence, skewness and attenuated backscatter coefficient	Manninen et al., 2018
Attenuated backscatter coefficient	Telescope focus function	Pentikainen et al., 2020

Doppler lidar toolbox: DL_toolbox (Markus Kayser)

The Doppler Lidar toolbox[1] developed and maintained by the German Weather Service in Lindenberg serves the community's demand for automatic processing of wind data. With its help operators are able to generate standardized and quality controlled level 2 (LV2) wind products for the two most common DL-architectures: The Halo Photonics Streamline-type by Lumibird and the WindCube Scan-type by Vaisala, formerly Leosphere. Possible configurations are listed in Table 4.

Table 4: Configuration options for Streamline and WindCube Scan lidars.

System	SCAN_TYPE	LV1	LV2	Quicklooks
Streamline	VAD UserX	yes	yes	LV1 / LV2
Streamline	DBS UserX	yes	yes	LV1 / LV2
Streamline	Stare	yes	no	LV1
Streamline	RHI	yes	no	no
WindCube Scan	fixed_VAD fixed_VAD_TP VAD VAD_TP	yes	yes	LV1 / LV2
WindCube Scan	DBS DBS_TP	yes	yes	LV1 / LV2
WindCube Scan	fixed/Stare fixed_TP/Stare_TP	yes	no	LV1
WindCube Scan	RHI RHI_TP	yes	no	no
WindCube Scan	PPI PPI_TP	yes	no	no

This Python software package is originally designed to facilitate data processing of Streamline systems. Through PROBE's collaborative work approach, the latest version was made applicable to WindCube Scan systems. The user controls processing with a customizable configuration file from the command line. This way, operators can implement automatic DL-processing operationally within their accustomed environment.

To derive the mean wind using DLs, the DL toolbox uses a best-practice VAD-variant, which has proven to be particularly efficient over years of testing at the Meteorological Observatory Lindenberg. The variant used in Lindenberg is described in Päschke et al. (2015) and Teschke and Lehmann (2017). This method allows for a simple calculation of uncertainties as well as efficient quality control via common fit parameters, namely the coefficient of determination, R^2, and the condition number of the algebraic least-squares regression, CN. In addition, the processing utilizes the minimum number of directions available for the calculation as a consistency criterion. For example, using a VAD with 24 LOS, setting the consistency criterion to 12 assures that at least 50 percent of the 24 LOS are used for the wind calculation. Additionally, the user can choose and combine two a-priori filter methods: the common

[1] DWD's Doppler lidar processing toolbox is a freely available python-based software,
link: https://github.com/mkay-atm/dl_toolbox.
For more details, please see VMG Report – User Guide for Doppler Lidar Toolbox (Kayser, 2024) and VMG Report – Testing of DL_toolbox for WindCube lidars (Preissler et al., 2024).

approach of SNR-thresholding or the consensus method, based on the random sample consensus (Fischler and Bolles, 1981), which was successfully implemented for radar wind profilers in the past.

Part 5 References

Bertonasco, E. and Kayser, M.: Test of Doppler lidar configurations for wind retrieval, PROBE COST action Virtual Mobility Grant report, doi: 10.5281/zenodo.10993087, 2024.

Bonin, T. A., Choukulkar, A., Brewer, W. A., Sandberg, S. P., Weickmann, A. M., Pichugina, Y. L., Banta, R. M., Oncley, S. P., and Wolfe, D. E.: Evaluation of turbulence measurement techniques from a single Doppler lidar, Atmos. Meas. Tech., 10, 3021–3039, https://doi.org/10.5194/amt-10-3021-2017, 2017.

Bonin, T. A., Carroll, B. J., Hardesty, R. M., Brewer, W. A., Hajny, K., Salmon, O. E., and Shepson, P. B.: Doppler Lidar Observations of the Mixing Height in Indianapolis Using an Automated Composite Fuzzy Logic Approach, J. Atmos. Oceanic Technol., 35, 473–490, https://doi.org/10.1175/JTECH-D-17-0159.1, 2018.

Calhoun, R., Heap, R., Princevac, M., Newsom, R., Fernando, H., & Ligon, D.: Virtual Towers Using Coherent Doppler Lidar during the Joint Urban 2003 Dispersion Experiment, J. Appl. Meteorol. Climatol, 45(8), 1116-1126, https://journals.ametsoc.org/view/journals/apme/45/8/jam2391.1.xml, 2006

Céspedes, J., Kotthaus, S., Preissler, J., Toupoint, C., Thobois, L., Drouin, M.-A., Dupont, J.-C., Faucheux, A., and Haeffelin, M.: The Paris Low-Level Jet During PANAME 2022 and its Impact on the Summertime Urban Heat Island, EGUsphere [preprint], https://doi.org/10.5194/egusphere-2024-520, 2024.

Debnath, M., Iungo, G. V., Ashton, R., Brewer, W. A., Choukulkar, A., Delgado, R., Lundquist, J. K., Shaw, W. J., Wilczak, J. M., and Wolfe, D.: Vertical profiles of the 3-D wind velocity retrieved from multiple wind lidars performing triple range-height-indicator scans, Atmos. Meas. Tech., 10, 431–444, https://doi.org/10.5194/amt-10-431-2017, 2017

Fischler, M. A., and Bolles, R. C.: Random Sample Consensus: A Paradigm for Model Fitting with Applications to Image Analysis and Automated Cartography. Communications of the ACM, 24(6):381–395. https://doi.org/10.1145/358669.358692, 1981.

Gryning, S. E., and Floors, R.: Carrier-to-noise-threshold filtering on off-shore wind lidar measurements. Sensors (Switzerland), 19(3). https://doi.org/10.3390/s19030592, 2019

Harvey, N. J., Hogan, R. J., and Dacre, H. F.: A method to diagnose boundary-layer type using Doppler lidar, Quart. J. Roy. Meteor. Soc.,139, 1681–1693, https://doi.org/10.1002/qj.2068, 2013.

Hunt, B. R., Kostelich, E. J., & Szunyogh, I.. Efficient data assimilation for spatiotemporal chaos: A local ensemble transform Kalman filter. Physica D: Nonlinear Phenomena, pp. 230,112-126. 2007.

Kayser, M.: PROBE COST action Virtual Mobility Grant report, doi: 2024.

Krishnamurthy, R., Newsom, R. K., Berg, L. K., Xiao, H., Ma, P. L., and Turner, D. D.: On the estimation of boundary layer heights: A machine learning approach, Atmos. Meas. Tech., 14, 4403–4424, https://doi.org/10.5194/AMT-14-4403-2021, 2021.

Lane S.E., J. F. Barlow, C. R. Wood: An assessment of a three-beam Doppler lidar wind profiling method for use in urban areas. J. WindEng. Ind. Aerodyn. 119, 53–59, 2013.

Manninen, A., Marke, T., Tuononen, M., and O'Connor, E.: Atmospheric boundary layer classification with Doppler lidar, J. Geophys. Res. Atmos., 123, 8172–8189, https://doi.org/10.1029/2017JD028169, 2018.

Manninen, A. J., O'Connor, E. J., Vakkari, V., and Petäjä, T.: A generalised background correction algorithm for a Halo Doppler lidar and its application to data from Finland, Atmos. Meas. Tech., 9, 817–827, https://doi.org/10.5194/amt-9-817-2016, 2016.

Merker, C., Regenass, D., & Leuenberger, D. EMER-Met StArt Project Report Annex 2: TP 2 Data Assimilation Final Report. Zürich: MeteoSwiss,2022

O'Connor, E. J., Illingworth, A. J., and Hogan, R. J.: A Technique for Autocalibration of Cloud Lidar, J. Atmos. Oceanic Technol., 21, 777–786, 2004.

O'Connor, E. J., Illingworth, A. J., Brooks, I. M., Westbrook, C. D., Hogan, R. J., Davies, F., and Brooks, B. J.: A Method for Estimating the Turbulent Kinetic Energy Dissipation Rate from a Vertically Pointing Doppler Lidar, and Independent Evaluation from Balloon-Borne In Situ Measurements, J. Atmos. Oceanic Technol., 27, 1652–1664, https://doi.org/10.1175/2010JTECHA1455.1, 2010.

Päschke, E., Leinweber, R., and Lehmann, V.: An assessment of the performance of a 1.5 µm Doppler lidar for operational vertical wind profiling based on a 1-year trial, Atmos. Meas. Tech., 8, 2251–2266, https://doi.org/doi:10.5194/amt-8-2251-2015, 2015.

Pearson, G.N., Davies, F., and Collier, C.: An analysis of the performance of the ufam pulsed Doppler lidar for observing the boundary layer. J. Atmos. Ocean. Technol, 26(2):240–250, 2009. doi: 10.1175/2008JTECHA1128.1.

Pearson, G-N- and Eacock, J. R.: Fiber-based coherent pulsed Doppler lidar for atmospheric monitoring. In Upendra N. Singh, editor, Lidar Remote Sensing for Industry and Environment Monitoring II, volume 4484, pages 51 – 57. International Society for Optics and Photonics, SPIE, 2002. doi: 10.1117/12.452799.

Pentikäinen, P., O'Connor, E. J., Manninen, A. J., and Ortiz-Amezcua, P.: Methodology for deriving the telescope focus function and its uncertainty for a heterodyne pulsed Doppler lidar, Atmos. Meas. Tech., 13, 2849–2863, https://doi.org/10.5194/amt-13-2849-2020, 2020.

Pichugina, Y. L., Banta, R. M., Brewer, W. A., Sandberg, S. P., & Hardesty, R. M.: Doppler Lidar–Based Wind-Profile Measurement System for Offshore Wind-Energy and Other Marine Boundary Layer Applications, J. Appl. Meteorol. Climatol, 51(2), 327-349, https://journals.ametsoc.org/view/journals/apme/51/2/jamc-d-11-040.1.xml, 2012

Pitter, M., Slinger, C., and Harris, M.: Introduction to continuous-wave Doppler lidar, Chap. 5, in: Remote Sensing for Wind Energy, edited by: Peña, A., DTU Wind Energy-E-Report-0084(EN), available at: https://orbit.dtu.dk/en/publications/remote-sensing-for-wind-energy-4 (last access: 13 January 2021), 2015.

Preissler, J., Kayser, M., Hervo, M. and Rüfenacht, R.: Testing of DL_toolbox for WindCube lidars, PROBE COST action Virtual Mobility Grant report, doi: 10.5281/zenodo.10792608, 2024.

Regenass, D. and Kaufmann, P., Assimilation of Wind Profiler Data at Basel, MeteoSwiss report, 2022

Reitebuch, O., in Schumann, U. (ed.), Atmospheric Physics, Chap. 30, Research Topics in Aerospace, Springer-Verlag Berlin Heidelberg, doi: 10.1007/978-3-642-30183-4_30, 2012

Schraff, C., Hendrik, R., Schrodin, A., Schomburg, A., Stephan, K., Periáñez, A., & Potthast, R. Kilometre-scale ensemble data assimilation for the COSMO model. Quarterly Journal of the Royal Meteorological Society, pp. 142, 1453-1472, 2014

Schween, J. H., Hirsikko, A., Löhnert, U., Crewell, S., and Iek, T.: Mixing-layer height retrieval with ceilometer and Doppler lidar : from case studies to long-term assessment, Atmos. Meas. Tech., pp. 3685–3704, https://doi.org/10.5194/amt-7-3685-2014, 2014

Smalikho, I. N. and Banakh, V. A.: Measurements of wind turbulence parameters by a conically scanning coherent Doppler lidar in the atmospheric boundary layer, Atmos. Meas. Tech., 10, 4191–4208, https://doi.org/10.5194/amt-10-4191-2017, 2017.

Teschke, G. and Lehmann, V.: Mean wind vector estimation using the velocity–azimuth display (VAD) method: an explicit algebraic solution, Atmos. Meas. Tech., 10, 3265–3271, https://doi.org/10.5194/amt-10-3265-2017, 2017.

Tucker, S. C., Senff, C. J., Weickmann, A. M., Brewer, W. A., Banta, R. M., Sandberg, S. P., Law, D. C., and Hardesty, R. M.:Doppler lidar estimation of mixing height using turbulence, shear, and aerosol profiles, J. Atmos. Oceanic Technol., 26, 673–688, https://doi.org/10.1175/2008JTECHA1157.1, 2009.

Tuononen, M., O'Connor, E. J., Sinclair, V. A., and Vakkari, V.: Low-level jets over Utö, Finland, based on Doppler lidar observations, J. Appl. Meteor. Climatol., 56, 2577–2594, https://doi.org/doi:10.1175/JAMC-D-16-0411.1, 2017.

Vakkari, V., O'Connor, E. J., Nisantzi, A., Mamouri, R. E., and Hadjimitsis, D. G.: Low-level mixing height detection in coastal locations with a scanning Doppler lidar, Atmos. Meas. Tech., 8, 1875–1885, https://doi.org/10.5194/amt-8-1875-2015, 2015.

Vakkari, V., Manninen, A. J., O'Connor, E. J., Schween, J. H., van Zyl, P. G., and Marinou, E.: A novel post-processing algorithm for Halo Doppler lidars, Atmos. Meas. Tech., 12, 839–852, https://doi.org/10.5194/amt-12-839-2019, 2019.

Appendix A Low level jets

The Paris Low-Level Jet During PANAME 2022 and its Impact on the Summertime Urban Heat Island (Jonnathan Céspedes)

The Low-Level Jet (LLJ) and the Urban Heat Island (UHI) are common nocturnal phenomena in the atmospheric boundary layer. While the canopy layer UHI has been studied extensively, interactions of the LLJ and the urban atmosphere in general (and the UHI in particular) have received less attention. In the framework of the PANAME initiative in the Paris region, continuous measurements of wind speed and vertical velocity profiles were recorded with two Doppler Wind Lidars (DWL) - for the first time allowing for a detailed investigation of the summertime LLJ characteristics in the region. Jets are detected for 70% of the examined nights, often simultaneously at an urban (QUALAIR-SU) and a suburban site (SIRTA) highlighting the LLJ regional spatial extent. Emerging at around sunset, the mean LLJ duration is ~10 h, the mean wind speed is ~9 m/s, and the average core height is 400 m above the city. For many jets, results show signatures in the temporal evolution that indicate that the inertial oscillation mechanism plays a role in the jet development: a clockwise veering of the wind direction and a rapid acceleration followed by a slower deceleration. The LLJ core wind shear induces variance in the vertical velocity (σ2w) above the urban canopy layer. It is shown that σ2w is a powerful indicator for the air temperature spatial contrasts as UHI intensity decreases exponentially with increasing σ2w and strong values only occur when σ2w is very weak. This study demonstrates how DWL observations in cities provide valuable insights into near-surface processes relevant to human and environmental health.

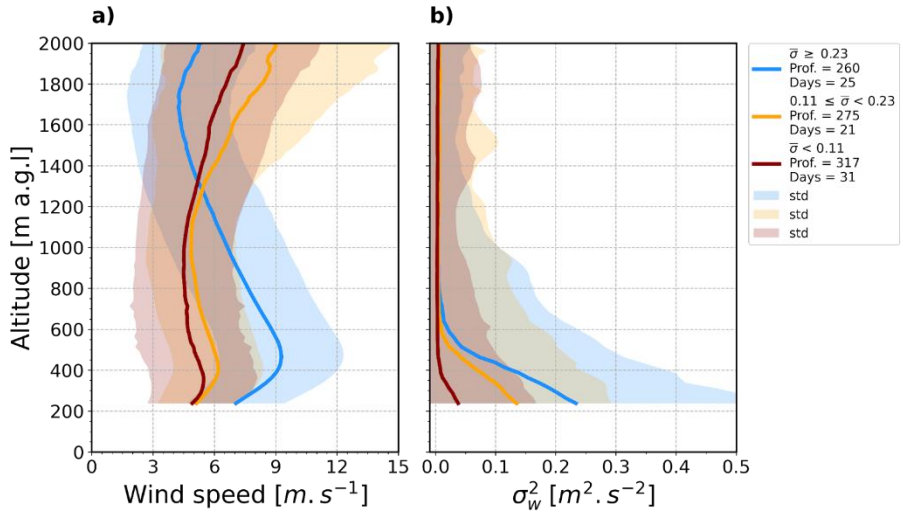

Figure A1. Mean profiles of a) horizontal wind speed and b) median profiles of vertical velocity variance σ2w. The solid lines represent the composite profile with all 30-min profiles detected as LLJ, and the shadows denote 1±std. Each panel presents the respective profiles for each σ2w class: red is low σ2w, orange is moderate and blue is strong σ2w.

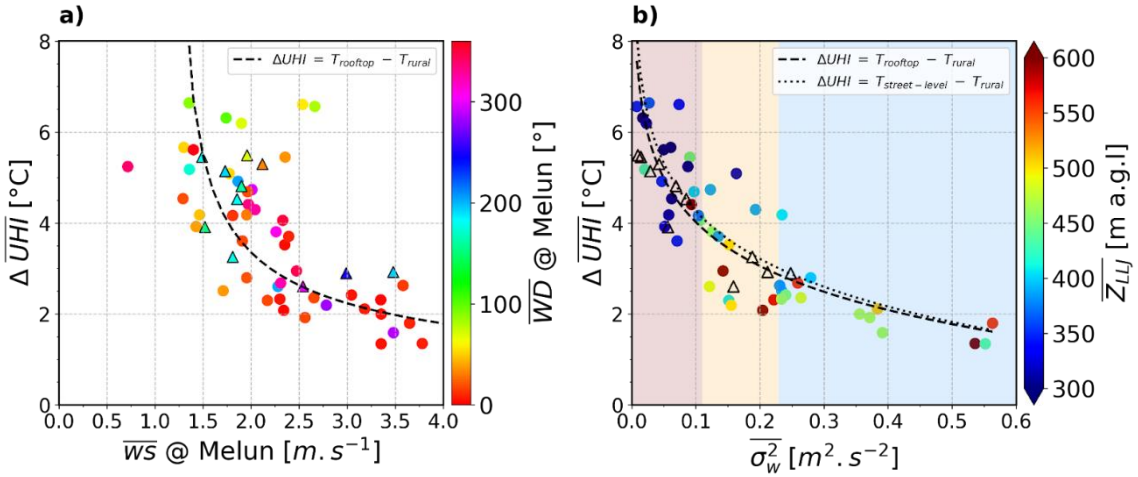

Figure A2. Relations between the nocturnal average of ΔUHI intensity for all cloud-free nights in the study period and a) 10m agl wind speed at Melun, the rural reference site. The dots are coloured by the surface wind direction at Melun. The dashed black curve is the best fit for the data:
y = 3((x−1.2)−0.5), and it follows the empirical relationship described by Oke (1973) b) the σ2w at 238 m agl, dots are colored by the LLJ core height above the ground surface. The dashed black curve represents the best non-linear fit found for the data collected in the Paris region and determines ΔUHI intensity with QUALAIR-SU data. The dotted black curve represents the same but using data collected by a surface-based station installed at Boulevard de Capucines for a shorter period. Both curves represent the equation: y = −1.39 log(x)+0.84. The background shading indicates the LLJ classes described in Section 3.2. In all subplots, dots, and triangles represent nights with and without LLJ events, respectively.